

Fluorescent Probes

Deutsche Ausgabe: DOI: 10.1002/ange.201609895
Internationale Ausgabe: DOI: 10.1002/anie.201609895

Near-Infrared Fluorescent Probe with New Recognition Moiety for Specific Detection of Tyrosinase Activity: Design, Synthesis, and Application in Living Cells and Zebrafish

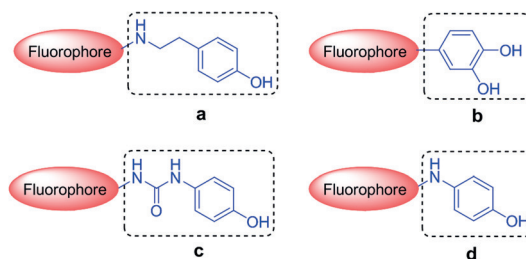
Xiaofeng Wu, Lihong Li, Wen Shi, Qiuyu Gong, and Huimin Ma*

Abstract: Fluorescence imaging of tyrosinase (a cancer biomarker) in living organisms is of great importance for biological studies. However, selective detection of tyrosinase remains a great challenge because current fluorescent probes that contain the 4-hydroxyphenyl moiety show similar fluorescence responses to both tyrosinase and some reactive oxygen species (ROS), thereby suffering from ROS interference. Herein, a new tyrosinase-recognition 3-hydroxybenzyloxy moiety, which exhibits distinct fluorescence responses for tyrosinase and ROS, is proposed. Using the recognition moiety, we develop a near-infrared fluorescence probe for tyrosinase activity, which effectively eliminates the interference from ROS. The high specificity of the probe was demonstrated by imaging and detecting endogenous tyrosinase activity in live cells and zebrafish and further validated by an enzyme-linked immunosorbent assay. The probe is expected to be useful for the accurate detection of tyrosinase in complex biosystems.

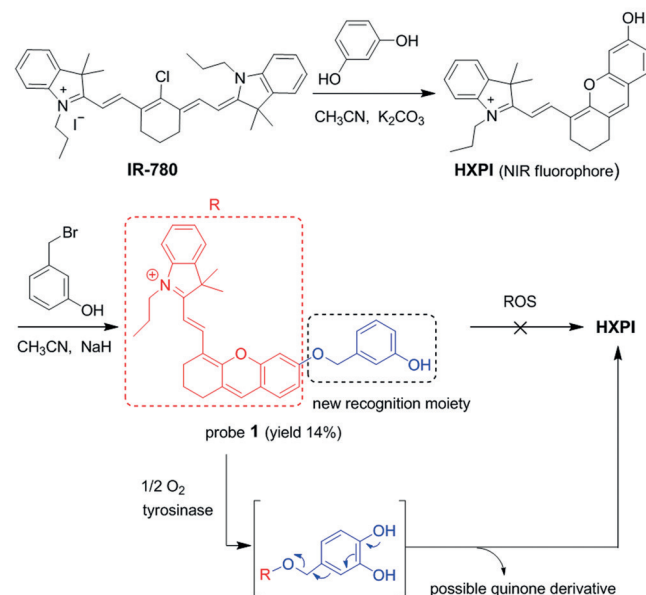
Tyrosinase, a copper-containing enzyme, can catalyze the hydroxylation and, subsequently, the further oxidation of a phenol unit to *ortho*-quinone in the presence of molecular oxygen.^[1] This enzyme is present widely in plants, animals, and microorganisms and is known as an important biomarker in melanoma cancer cells.^[1] Moreover, an abnormal level of tyrosinase may lead to vitiligo and Parkinson's disease.^[2] The detection of tyrosinase in living organisms is thus of great significance for clinical research.^[3]

Owing to their high sensitivity and unrivaled spatiotemporal sampling capability,^[4–7] fluorescence probes combined with confocal imaging techniques have drawn much attention for monitoring tyrosinase in living biosystems.^[5] However, sensitive and in particular selective detection of tyrosinase activity still remains a great challenge, because current fluorescent probes with the recognition moieties **a–d** (Figure 1A) show similar fluorescence responses to both tyrosinase and some reactive oxygen species (ROS) such as HOCl, H₂O₂, and ONOO[–],^[5,6] thereby suffering from the ROS

(A) Previous studies

Fluorescence of probes with previous recognition moieties (**a–d**) is interfered by ROS

(B) This study

Probe **1** with the following new recognition moiety eliminates the ROS interference

(C) Model compounds

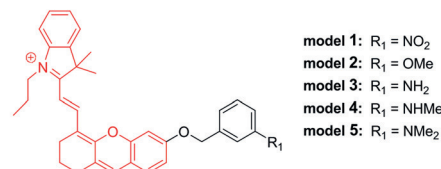


Figure 1. A) Previous studies. Traditional fluorescent probes with the recognition moieties (**a–d**) for tyrosinase. B) This study. Synthesis of probe **1** with a new recognition moiety, 3-hydroxybenzyloxy, and the proposed reaction mechanisms of probe **1** with tyrosinase and ROS. C) Model compounds **1–5**.

[*] X. F. Wu, Dr. L. H. Li, Prof. Dr. W. Shi, Dr. Q. Y. Gong, Prof. Dr. H. M. Ma
Beijing National Laboratory for Molecular Sciences, Key Laboratory of Analytical Chemistry for Living Biosystems, Institute of Chemistry, Chinese Academy of Sciences
Beijing 100190 (China)
E-mail: mahm@iccas.ac.cn
X. F. Wu, Prof. Dr. H. M. Ma
University of the Chinese Academy of Sciences
Beijing 100049 (China)

Supporting information for this article can be found under:
<http://dx.doi.org/10.1002/anie.201609895>.

interferences. The cross-responses may lead to inaccurate results, because HOCl and H₂O₂ are usually present at a relatively high concentration (about μM levels) in biosystems such as cancer cells.^[8]

To address this issue, we propose a new tyrosinase-recognition moiety, 3-hydroxybenzyloxy, in which the presence of the unique 3-hydroxy (instead of 4-hydroxy) group facilitates the hydroxylation at the 4-position vacancy by tyrosinase but not by ROS, and the resulting hydroxylation unit would be spontaneously removed by the subsequent 1,6-rearrangement–elimination. With this in mind, by incorporating the recognition moiety 3-hydroxybenzyloxy into a stable hemicyanine skeleton,^[9] we developed a near-infrared (NIR) fluorescence probe **1** (Figure 1B) for tyrosinase activity. Moreover, because the copper of the tyrosinase active site coordinates directly with phenolic substrates,^[1a] we prepared and compared various model compounds bearing other 3-substituents (**1–5**; Figure 1C) to show that the 3-hydroxy group is necessary in the recognition moiety.

Probe **1** and model compounds **1–5** (Figure 1 and the Supporting Information, Scheme S1) were prepared by incorporating different 3-substituted benzyloxy moieties into a NIR fluorophore HXPI.^[9,10] The detailed synthetic steps and characterization of probe **1** and model compounds **1–5** are given in the Supporting Information, Figures S1–S12 and Table S1.

The reactivity of probe **1** and models **1–5** toward tyrosinase was investigated. As shown in Figure S13 (Supporting Information), probe **1** shows a broad absorption band with peaks at 600 and 650 nm, and its reaction with tyrosinase leads to the broadening of the peak at 650 nm to about 670 nm, accompanied by a distinct color change from purple to blue (see the inset in the Supporting Information, Figure S13A). Most notably, reaction of probe **1** with tyrosinase produces a large fluorescence off-on response at 708 nm (Figure S13B); under the same conditions (Figure 2A), however, the model compounds only show a small fluorescence change, except for the moderate response from model **4**. The reason for this phenomenon is rather complicated, but a feasible explanation may be that the copper of the tyrosinase active site is favorable for direct coordination with phenolic substrates.^[1a] The above result clearly supports our hypothesis that 3-hydroxy is crucial in the proposed recognition moiety.

Reaction conditions of probe **1** with tyrosinase were optimized, including pH, temperature, and time. As shown in the Supporting Information, Figure S14, the fluorescence of probe **1** itself is not largely affected by the change of pH from 6.5 to 7.5 and temperature from 25 to 42 °C, and the maximum fluorescence enhancement of probe **1** reacting with tyrosinase is achieved at about pH 7.4 and 37 °C, as an enzyme usually functions well under normal physiological conditions. Time course studies showed that the fluorescence intensity reached a plateau in about 3 h (Supporting Information, Figure S15). Under the optimized conditions (reaction in pH 7.4 media at 37 °C for 3 h), a good correlation with a linear equation of $\Delta F = 3.25 \times C(\text{U mL}^{-1}) + 6.40$ ($R = 0.991$) was obtained in the tyrosinase activity range of 0–80 U mL^{−1} (Figure 2B,C), and the detection limit ($k = 3$)^[11] was determined to be

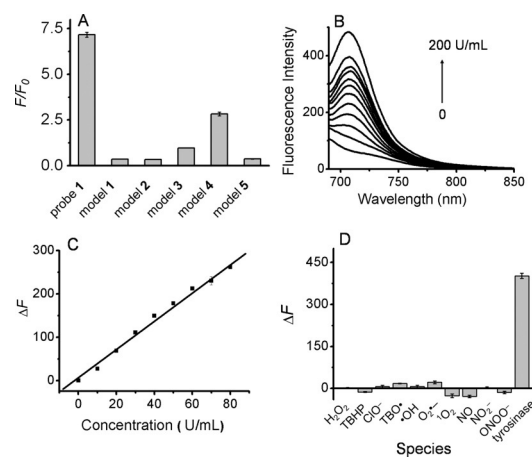


Figure 2. A) Fluorescence responses of probe **1** and model compounds **1–5** (each 5 μM) to tyrosinase (200 U mL^{−1}). Reaction was performed in PBS (pH 7.4) at 37 °C for 3 h. F/F_0 is the ratio of fluorescence intensity after (F) and before (F_0) reaction. B) Fluorescence response of probe **1** (5 μM) to tyrosinase at different concentrations (0–200 U mL^{−1}). C) Linear relationship between ΔF and the tyrosinase concentration (0–80 U mL^{−1}). ΔF is the fluorescence intensity difference after and before reaction. D) Fluorescence responses of probe **1** (5 μM) to ROS (H₂O₂, TBHP, ClO[−], TBO[•], [•]OH, O₂^{•−}, ¹O₂, NO, NO₂[−], and ONOO[−]; 100 μM each) and tyrosinase (200 U mL^{−1}). $\lambda_{\text{ex/em}} = 670/708$ nm.

2.76 U mL^{−1}. The kinetic parameters such as the Michaelis constant (K_m) and maximum of initial reaction rate (V_{max}) for the enzymatic cleavage reaction of probe **1** were found to be 156 μM and 4.58 $\mu\text{M min}^{-1}$ (Supporting Information, Figure S16), respectively.

Next, the selectivity of probe **1** was studied for tyrosinase over a series of ROS at both relatively high and low levels. As shown in Figure 2D and the Supporting Information, Figure S17, tyrosinase exhibits the largest fluorescence response, whereas the ROS even at a concentration much higher than their physiological levels do not significantly change the probe's fluorescence (within $\pm 10\%$). Moreover, the commonly co-existing biological substances tested, such as inorganic salts, glucose, vitamin C, vitamin B6, glycine, glutamic acid, cysteine, glutathione, creatinine, urea, and some enzymes, did not produce obvious fluorescence responses either (Supporting Information, Figure S18). Thus, the probe displays high specificity for tyrosinase.

To confirm the fluorescence response mechanism, the reaction products of probe **1** with tyrosinase were analyzed by both electrospray ionization (ESI) mass spectrometry and HPLC. As shown in the Supporting Information, Figure S19, reaction of probe **1** with tyrosinase generates a peak at m/z 412.3 [M]⁺ in the ESI mass spectrum, confirming the release of HXPI; under the same conditions, however, the formation of HXPI is not detected in the presence of various ROS, as depicted in the Supporting Information, Figure S20. Furthermore, HPLC analysis (Supporting Information, Figure S21) showed that upon reaction with tyrosinase, the peak at 8.17 min, which represents probe **1**, decreases greatly, accompanying the appearance of a new peak at 6.54 min, which is indicative of HXPI (curve C). The above results clearly

indicate that the fluorescence response results from the generation of HXPI. On the other hand, previous studies showed that, when ROS react with the fluorescent probes containing the hydroxyl recognition units for tyrosinase (Figure 1 A), it seems to preferably form a quinone derivative instead of a hydroxylated product.^[6] This behavior of ROS might also apply to probe **1**, but the resulting *meta*-quinone does not easily serve as a leaving group, suggesting that it is hard for ROS to produce a fluorescence response. In contrast, the special function of tyrosinase may cause the probe's hydroxylation at the 4-position vacancy, and the resulting hydroxylation unit readily undergoes a spontaneous 1,6-rearrangement–elimination (possibly leaving as a quinone derivative), thereby turning on the probe's fluorescence. These different reaction behaviors may be responsible for the high selectivity of the probe toward tyrosinase over ROS, as depicted in Figure 1 B.

Kojic acid, a versatile biological agent,^[12] may serve as not only a scavenger of ROS (for example, $\cdot\text{OH}$, $\text{O}_2^{\cdot-}$, and $^1\text{O}_2$)^[12a,b] but also an inhibitor of enzymes (for example, polyphenol oxidases, xanthine oxidase, and amino acid oxidases).^[12c–e] The degree and mode of these scavenging or inhibiting actions also depend on several factors such as concentration and biological environment.^[12a,c] Nevertheless, one of the most important functions of kojic acid is to serve as a standard inhibitor of tyrosinase.^[12f] Thus, the effect of kojic acid was examined to further demonstrate the fluorescence changes of the probe resulting from the action of tyrosinase. As compared to the control, addition of kojic acid to a solution containing tyrosinase and probe **1** decreases the measured fluorescence, and higher concentrations of kojic acid lead to a greater decrease in the fluorescence intensity (Supporting Information, Figure S22). On the other hand, the inhibitor of kojic acid shows nearly no effect on the fluorescence of both fluorophore HXPI and probe **1** when no tyrosinase is present (Supporting Information, Figure S23). Therefore, the above findings demonstrate that the presence of kojic acid inhibits the tyrosinase activity, and the fluorescence change of probe **1** reacting with tyrosinase indeed arises from the enzymatic cleavage reaction. Moreover, probe **1** displays good biocompatibility (Supporting Information, Figure S24).

Owing to its high specificity for tyrosinase, probe **1** is anticipated to be capable of accurately detecting the enzyme activity in living cells or organisms. To demonstrate this potential, murine melanoma B16 cells were used as a model, because they overexpress tyrosinase.^[13] As depicted in Figure 3 A, B16 cells themselves show an extremely low background fluorescence (image a), which benefits from the NIR excitation wavelength of the probe. However, the B16 cells treated with probe **1** exhibit strong fluorescence (image b), suggesting a good cell-permeability for probe **1** and its possible reaction with tyrosinase in the cells. To verify that the fluorescence change was caused by tyrosinase, kojic acid (inhibitor) was used to pretreat the cells, and the pretreated cells generated a markedly lower fluorescence (image c), in which the relative pixel intensity decreases by about 50% (compare the intensity values of b and c in Figure 3 B). This indicates that the fluorescence enhancement in B16 cells does result from the endogenous tyrosinase. Importantly, both

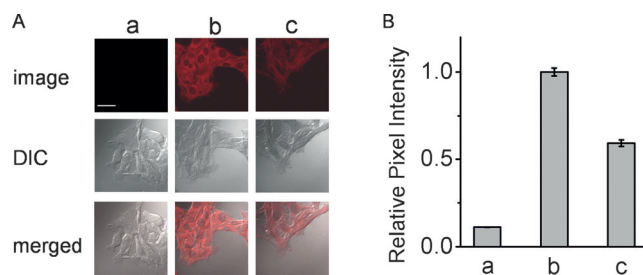


Figure 3. A) Confocal fluorescence images of B16 cells: a) cells only (control); b) cells incubated with probe **1** ($5\ \mu\text{M}$) for 3 h; c) cells pretreated with kojic acid ($200\ \mu\text{M}$) for 2 h and then incubated with probe **1** ($5\ \mu\text{M}$) for 3 h. The differential interference contrast (DIC) and merged images of the corresponding samples are shown in the middle and bottom rows, respectively. Scale bar = $30\ \mu\text{m}$. B) Relative pixel intensity ($n=3$) from images (a)–(c) in (A). The pixel intensity from image (b) is defined as 1.0.

siRNA-transfected B16 and HeLa cells with the inhibited expression of tyrosinase, as further evidenced by the enzyme-linked immunosorbent assay (ELISA), showed a greatly decreased intracellular fluorescence (Supporting Information, Figure S25), clearly indicating that this intracellular fluorescence change reflects the alteration of the relative tyrosinase activity. Interestingly, no obvious fluorescence increase was observed outside the cells (Figure 4 A), and no mass peak of HXPI (Supporting Information, Figure S26) was

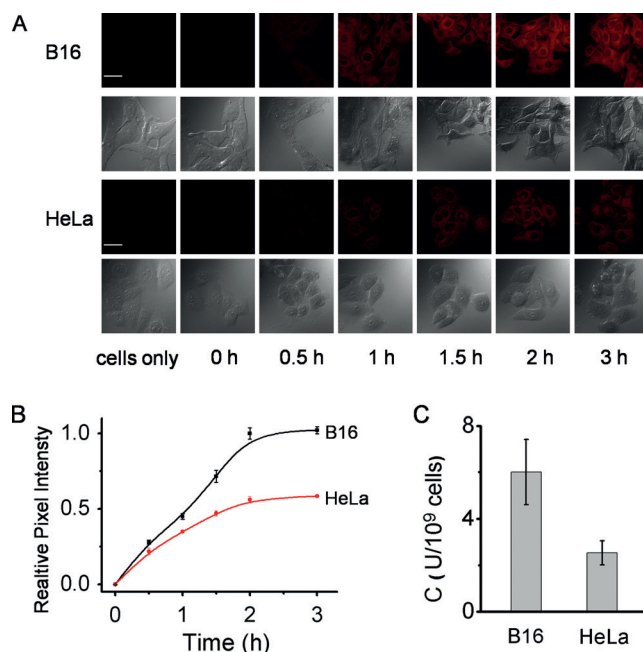


Figure 4. A) Fluorescence and DIC images of B16 and HeLa cells. The cells were incubated with probe **1** ($5\ \mu\text{M}$) at 37°C for different periods of time (0, 0.5, 1.0, 1.5, 2.0, and 3.0 h). Scale bar = $30\ \mu\text{m}$. B) The plots of the relative pixel intensity of the fluorescence images from 0–3 h in (A) versus time. Note that the pixel intensity of the images from 0–3 h was obtained by subtracting the intensity from the control (cells only), and the pixel intensity from the 3-h image of B16 cells is defined as 1.0. C) The activity of tyrosinase in B16 and HeLa cells determined by ELISA kits. The results are expressed as the mean \pm standard deviation of three separate measurements.

detected in the media containing the probe-loaded cells, implying a good retainability of the released HXPI inside the cells under the present conditions. Furthermore, probe **1** was used to distinguish the relative levels of tyrosinase in different cell lines such as B16 and HeLa cells under the same imaging conditions. As shown in Figure 4, fluorescence linearly increases with time within about 2 h for the two kinds of cells, and the slope of the time-dependent increase of fluorescence in B16 cells is about 1.6-fold larger than that in HeLa cells (Figure 4B), suggesting that the tyrosinase level in B16 cells might be about 1.6-fold higher than that in HeLa cells (assuming that the reaction properties of the probe in the two cell lines are equal). This result is roughly consistent with that (about a 2-fold increase) determined by ELISA (Figure 4C). Note that the small inconsistency between the two methods might be due to the rather low level of intracellular tyrosinase (Figure 4C) and/or the different reactivity of the probe in the two cell lines. The above study demonstrates that probe **1** can be used to visualize the relative tyrosinase activity in different living cells.

Because of the advantages of NIR,^[4a] probe **1** was further investigated to image the tyrosinase activity in living zebrafish. As shown in Figure 5A, 3-day-old zebrafish display nearly no background fluorescence (image a), but the probe-loaded zebrafish produce strong fluorescence (image b). This implies that the probe is tissue-permeable and zebrafish contain a detectable tyrosinase level, which was determined by ELISA (see Supporting Information) to be about 20 mU per 3-day-old zebrafish. Interestingly, the fluorescence in the zebrafish is not uniformly distributed, and the zebrafish yolk sac shows rather weak fluorescence. Our previous study indicated that the fluorophore of HXPI is distributed

throughout almost the whole body of zebrafish.^[10b] Therefore, the weak fluorescence from the zebrafish yolk sac may reflect a low abundance of tyrosinase. This phenomenon has not been reported to the best of our knowledge. Moreover, an inhibition experiment was performed to further demonstrate the fluorescence generation from probe **1** in zebrafish resulting from tyrosinase activity. As seen from Figure 5, the fluorescence intensity from zebrafish decreases gradually with increasing kojic acid concentration; for example, 200 and 500 μM of kojic acid causes a significant decrease of the fluorescence by about 60 % and 80 % (Figure 5B), respectively. The above results indicate that probe **1** is capable of monitoring the endogenous tyrosinase activity in living bodies.

In summary, we have proposed a new tyrosinase-recognition 3-hydroxybenzyloxy moiety, which shows different reaction mechanisms for tyrosinase and ROS; the former leads to the removal of the recognition moiety and the latter do not. By engineering a 3-hydroxybenzyloxy moiety into a stable hemicyanine skeleton, we have developed probe **1**, which displays a specific NIR fluorescence off-on response to tyrosinase rather than ROS, and thus overcomes ROS interference. The high specificity of probe **1** permits the accurate detection of the tyrosinase activity in live cells and zebrafish, as further validated by ELISA. We believe that probe **1** may be useful for monitoring the change of endogenous tyrosinase activity in biosystems.

Acknowledgements

This work is supported by grants from the 973 Program (Nos. 2015CB932001 and 2015CB856301), the NSF of China (Nos. 21535009, 21675159, 21435007, and 21321003), and the Chinese Academy of Science (XDB14030102).

Keywords: analytical methods · fluorescent probes · reactive oxygen species · recognition moiety · tyrosinase

How to cite: *Angew. Chem. Int. Ed.* **2016**, 55, 14728–14732
Angew. Chem. **2016**, 128, 14948–14952

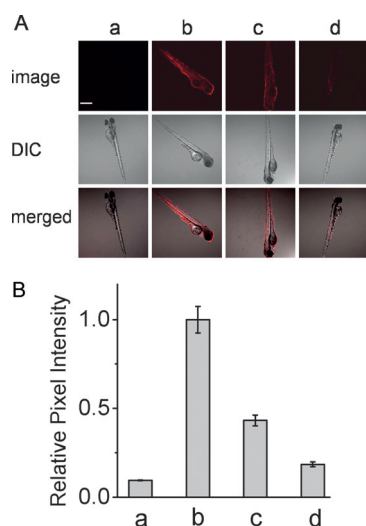


Figure 5. A) Fluorescence images of 3-day-old zebrafish: a) Zebrafish only, b) zebrafish incubated with probe **1** ($5 \mu\text{M}$) for 3 h, zebrafish pretreated with c) 200 μM and d) 500 μM kojic acid for 2 h and then incubated with probe **1** ($5 \mu\text{M}$) for 3 h. The top, middle, and bottom rows represent the fluorescence, DIC, and merged images of zebrafish, respectively. Scale bar = 500 μm . B) Relative pixel intensity measurements ($n=3$) from images (a)–(d) in (A) were obtained by using the Olympus software. The pixel intensity from image (b) is defined as 1.0.

- [1] a) E. I. Solomon, U. M. Sundaram, T. E. Machonkin, *Chem. Rev.* **1996**, 96, 2563–2605; b) L. M. Mirica, M. Vance, D. J. Rudd, B. Hedman, K. O. Hodgson, E. I. Solomon, T. D. P. Stack, *Science* **2005**, 308, 1890–1892; c) M. Jimenez, K. Kameyama, W. L. Maloy, Y. Tomita, V. J. Hearing, *Proc. Natl. Acad. Sci. USA* **1988**, 85, 3830–3834; d) J. Y. Lin, D. E. Fisher, *Nature* **2007**, 445, 843–850; e) E. Solem, F. Tuzcek, H. Decker, *Angew. Chem. Int. Ed.* **2016**, 55, 2884–2888; *Angew. Chem.* **2016**, 128, 2934–2938; f) M. Rolff, J. Schottenheim, H. Decker, F. Tuzcek, *Chem. Soc. Rev.* **2011**, 40, 4077–4098, and references therein.
- [2] a) I. Tessari, M. Bisaglia, F. Velle, B. Samori, E. Bergantino, S. Mammi, L. Bubacco, *J. Biol. Chem.* **2008**, 283, 16808–16817; b) T. Hasegawa, A. Treis, N. Patenge, F. C. Fiesel, W. Springer, P. J. Kahle, *J. Neurochem.* **2008**, 105, 1700–1715.
- [3] a) J. C. Espin, J. Tudela, F. Garcia-Canovas, *Anal. Biochem.* **1998**, 259, 118–126; b) R. Freeman, J. Elbaz, R. Gill, M. Zayats, I. Willner, *Chem. Eur. J.* **2007**, 13, 7288–7293; c) Q. L. Xu, J. Y. Yoon, *Chem. Commun.* **2011**, 47, 12497–12499; d) X. L. Zhou, J.

- Hu, Z. H. Zhao, M. J. Sun, X. Q. Chi, X. M. Wang, J. H. Gao, *Small* **2015**, *11*, 862–870.
- [4] a) X. H. Li, X. H. Gao, W. Shi, H. M. Ma, *Chem. Rev.* **2014**, *114*, 590–659; b) X. F. Wu, L. H. Li, W. Shi, Q. Y. Gong, X. H. Li, H. M. Ma, *Anal. Chem.* **2016**, *88*, 1440–1446.
- [5] a) T. I. Kim, J. Park, S. Park, Y. Choi, Y. Kim, *Chem. Commun.* **2011**, *47*, 12640–12642; b) S. Y. Yan, R. Huang, C. C. Wang, Y. M. Zhou, J. Q. Wang, B. S. Fu, X. C. Weng, X. Zhou, *Chem. Asian J.* **2012**, *7*, 2782–2785; c) J. Zhou, W. Shi, L. H. Li, Q. Y. Gong, X. F. Wu, X. H. Li, H. M. Ma, *Anal. Chem.* **2016**, *88*, 4557–4564.
- [6] a) J. Kim, Y. Kim, *Analyst* **2014**, *139*, 2986–2989; b) F. B. Yu, P. Li, P. Song, B. S. Wang, J. Z. Zhao, K. L. Han, *Chem. Commun.* **2012**, *48*, 4980–4982; c) W. Zhang, P. Li, F. Yang, X. F. Hu, C. Z. Sun, W. Zhang, D. Z. Chen, B. Tang, *J. Am. Chem. Soc.* **2013**, *135*, 14956–14959; d) H. X. Zhang, J. Liu, Y. Q. Sun, Y. Y. Huo, Y. H. Li, W. Z. Liu, X. Wu, N. S. Zhu, Y. W. Shi, W. Guo, *Chem. Commun.* **2015**, *51*, 2721–2724; e) T. Peng, N. K. Wong, X. M. Chen, Y. K. Chan, D. H. H. Ho, Z. N. Sun, J. J. Hu, J. G. Shen, H. El-Nezami, D. Yang, *J. Am. Chem. Soc.* **2014**, *136*, 11728–11734.
- [7] a) R. Gill, R. Freeman, J. P. Xu, I. Willner, S. Winograd, I. Shweky, U. Banin, *J. Am. Chem. Soc.* **2006**, *128*, 15376–15377; b) C. C. Wang, S. Y. Yan, R. Huang, S. Feng, B. S. Fu, X. C. Weng, X. Zhou, *Analyst* **2013**, *138*, 2825–2828; c) Y. Teng, X. F. Jia, J. Li, E. K. Wang, *Anal. Chem.* **2015**, *87*, 4897–4902.
- [8] a) M. V. Avshalumov, L. Bao, J. C. Patel, M. E. Rice, *Antioxid. Redox Signaling* **2006**, *2*, 219–231; b) H. Hagen, P. Marzenell, E. Jentsch, F. Wenz, M. R. Veldwijk, A. Mokhir, *J. Med. Chem.* **2012**, *55*, 924–934; c) Y. W. Yap, M. Whiteman, N. S. Cheung, *Cell. Signalling* **2007**, *19*, 219–228.
- [9] Q. Q. Wan, S. M. Chen, W. Shi, L. H. Li, H. M. Ma, *Angew. Chem. Int. Ed.* **2014**, *53*, 10916–10920; *Angew. Chem.* **2014**, *126*, 11096–11100.
- [10] a) L. H. Li, Z. Li, W. Shi, X. H. Li, H. M. Ma, *Anal. Chem.* **2014**, *86*, 6115–6120; b) Z. Li, X. Y. He, Z. Wang, R. H. Yang, W. Shi, H. M. Ma, *Biosens. Bioelectron.* **2015**, *63*, 112–116.
- [11] Q. Q. Wan, Y. C. Song, Z. Li, X. H. Gao, H. M. Ma, *Chem. Commun.* **2013**, *49*, 502–504.
- [12] a) Y. Niwa, H. Akamatsu, *Inflammation* **1991**, *15*, 303–315; b) A. J. Gomes, C. N. Lunardi, S. Gonzalez, A. C. Tedesco, *Braz. J. Med. Biol. Res.* **2001**, *34*, 1487–1494; c) G. A. Burdock, M. G. Soni, I. G. Carabin, *Regul. Toxicol. Pharmacol.* **2001**, *33*, 80–101, and references therein; d) R. Saruno, F. Kato, T. Ikeno, *Agric. Biol. Chem.* **1979**, *43*, 1337–1338; e) J. R. Klein, N. S. Olsen, *J. Biol. Chem.* **1947**, *170*, 151–157; f) T. S. Chang, *Int. J. Mol. Sci.* **2009**, *10*, 2440–2475.
- [13] a) R. White, F. N. Hu, *J. Invest. Dermatol.* **1977**, *68*, 272–276; b) S. R. Harry, D. J. Hicks, K. I. Amiri, D. W. Wright, *Chem. Commun.* **2010**, *46*, 5557–5559.

Received: October 10, 2016

Published online: October 24, 2016